UNIVERSITY OF ILLINOIS

MAY 9 19 90

THIS IS TO CERTIFY THAT THE THESIS PREPARED UNDER MY SUPERVISION BY

Aline Christine Hoey

ENTITLED STUDIES OF MOLECULAR CLUSTERS USING

ROTATIONAL SPECTROSCOPY

IS APPROVED BY ME AS FULFILLING THIS PART OF THE REQUIREMENTS FOR THE

DEGREE OF Bachelor of Science in Chemistry

W. S. Benedict
Instructor in Charge

APPROVED: H. L. Strauss

HEAD OF DEPARTMENT OF Chemistry

O-1364

Studies of Molecular Clusters Using Rotational Spectroscopy

By

Aline Christine Hoey

Thesis

for the Degree of Bachelor of Science

in

Chemistry

College of Liberal Arts and Sciences

University of Illinois

Urbana, Illinois

1990

Table of Contents

ABSTRACT

Microwave rotational spectra for Ar/HF/DF and Ar (H_2O-HCN) have been observed with a pulsed nozzle Fourier transform method, using the Flygare-Balle Mark II Spectrometer. Several assignments were made for the Ar/HF/DF system, however none were conclusive. The Ar/H_2O/HCN system was studied in the same manner. The Ar (H_2O-HCN) trimer was assigned three rotational constants, A=3536 MHz, B=1845 MHz, and C=1218 MHz. Both μ_a and μ_b type transitions were observed, however the μ_b type transitions were considerably stronger. The deviation between observed and calculated transition frequencies were larger for the μ_a type transitions. This may be due to a coupling of internal rotation with molecular rotation with the major component of coupling along the a- inertial axis.

INTRODUCTION

The Ar/HF/DF system was studied over a large range of frequency. Many transitions were found and several were assigned to particular geometric species. The most promising species is the trimer system $Ar(DF)_2$.

The Ar/HF/DF system produces many clusters upon expansion, making the assignment of transitions difficult. The $Ar_nH(D)F$ clusters up to n=4 have been previously studied.[1,2,3,4,5] Generally they form an Ar_n cluster with the H(D)F equilibrium position along the main figure axis of the Ar . Some of the transitions were assigned to the n=5 trigonal bipyramidal structure, however, the larger the cluster the lower its concentration in the gas jet.

Some transitions were assigned to the $Ar(H(D)F)_2$ system. The $(H(D)F)_2$ dimers were previously studied.[6,7] The H(D)F's are at two different angles to the F--F axis in the dimer, allowing tunneling to occur in the homodimers. Tunneling occurs due to inversion of the two substituents. In this paper I will detail the continued searches and assignments done on the Ar/HF/DF system.

The $Ar/H_2O/HCN$ system was studied in the same manner. The ground vibronic structure of the H_2O-HCN dimer has previously been reported.[8] The dimer is effectively planar H_2O---HCN, with the O acting as the proton acceptor and the H from the HCN acting as the proton donor of the H-bond. The rotational spectrum consists only of μ_b type, R-branch transitions, indicating that the O--HCN is effectively linear.

Transitions of the Ar(H_2O-HCN) trimer were observed. The structure appears to be perturbed by the addition of an Ar allowing for both μ_a and μ_b type transitions. Rotational constants were calculated and the transitions fitted. The inertial defect was also calculated. The hfs of some transitions could be fitted, however, not all transitions could be fitted due to a dependence of the quadrupole interaction term on the rotational level.

EXPERIMENTAL

The microwave spectra were obtained using the Flygare-Balle Mark II spectrometer, which has previously been described[9,5]. A pulse of carrier gas seeded with the component gases is introduced into an evacuated cavity through a supersonic nozzle. The gas expands and cools to approximately 5K allowing small clusters to form. The clusters are hit with an adjustable microwave pulse. On resonance the sample is polarized and produces a free induction decay (FID) signal in the cavity. The signal is detected, digitized, accumulated and Fourier transformed producing the frequency spectrum. The Ar/HF/DF spectra were obtained with Ar (Linde) as a carrier gas. The concentrations for the search were 98% Ar, 1% HF and 1% DF with a backing pressure of approximately an atm. The observed transitions were optimized at different concentrations indicating the formation of several different clusters upon expansion.

The Ar-(H_2O- HCN) transitions were also observed in the same manner, using the Flygare-Balle Mark II spectrometer. However the gas handling system was improved. The gas handling system was computerized to achieve more accurate control of concentrations. The concentrations of Ar, H_2O, and HCN were 99.5, 0.25, and 0.25% respectively.

RESULTS AND ANALYSIS

The Ar/HF/DF system produces numerous clusters upon expansion, many of which have been studied previously. However an extended search led to the observation of many new transitions. The areas searched with Ar/HF/DF include 6001.3-6032.4, 5757-5923, 6059-6117, 6124.9-6129.2, 6212.2-6252.9, and 9500 9540 MHz. Other areas were also searched, however, with only one isotopic component, HF or DF. The lines found are summarized in Table I.

Many species and structures were analyzed and compared with these transitions, including an Ar_5 H(D)F trigonal bipyramid, Ar_4 H(D)F planar and bent rhombic,and Ar_3 H(D)F arrow structure. These structures were analyzed by predicting the geometry, obtaining rotational constants and calculating the spectrum including hfs. After comparison between the observed hfs and the calculated hfs all of the structures were eliminated as possibilities.

The hfs was calculated by evaluating the Hamiltonian including the spin-spin coupling term and the quadrupole term for the deuterated species. The spin-spin coupling and quadrupole interaction terms were calculated using the tensor method. The spin-spin coupling for free HF and DF were projected onto the inertial axis using the equation.

$$D_{xx} = D_o \ (1/2)\langle 3\cos^2\emptyset_{zx} - 1\rangle \qquad (1)$$

where D_{xx} is the spin-spin interaction term on the inertial axis (x=a,b,c), D_0 is the spin-spin interaction of free HF or DF and $\emptyset_{zx}$ is the angle between the molecular axis and the inertial axis that it is projected onto.

The hfs produced by the quadrupole interaction was calculated for the DF species in a similar manner, by projecting the tensor onto the inertial axis. The spin-spin coupling and quadrupole interaction tensors were assumed to be diagonal due to the symmetry along the Ar_n-H(D)F axis. The ICI fitting program was used to calculate the hyperfine structures, which were compared with observed hfs.

Several transitions were observed from Ar containing trimers with more than one H(D)F. The hyperfine structure and the required concentrations of H(D)F led to this conclusion. The transitions assigned to $Ar(DF)_2$ are listed in Table II.

The $(H(D)F)_2$ species have been characterized previously. They have a planar, bent geometry H-F---H-F, with the end H-F bent counterclockwise from the F---F axis by 63+/-6° and the inside H-F bent 10+/-6° the opposite way. For $Ar(H(D)F)_2$ structures the geometry is assumed to be essentially the same, however with an Ar attached. The location of the Ar is unknown and is the cause of difficulty in characterizing the species. It is possible that the addition of the Ar perturbs the structure of the dimer. Due to the predicted geometry, the homodimer species are expected to exhibit tunneling, which splits each transition into a pair. The three transitions found exhibit this type of hfs with a separation between

transition pairs of about 1 MHz. The tunneling splitting is included in Table II.

The 6010.89 and 6278.68 doublets exhibit similar hfs ranging over 65 and 106 khz and 72 and 94 KHz respectively. This observation supports the assignment of both transitions to the same type of dipole transition. The 9340.04 MHz line has a different hfs and a much stronger intensity, indicating that it arises from a different transition dipole. Other lines have been found that possibly arise from the same species. They are at 5981.11, 6692.75, and 9124.65 MHz respectively.

Tentative assignments were made for the observed transitions. Fitting programs were used to determine the rotational constants, A, B, and C. Finally, the spectrum was calculated assuming that μ_a, μ_b, and μ_c type transitions could occur. The assignments and the rotational constants are listed in Table III. Several of the assignments were immediately ruled out due to predicted strong transitions in previously searched areas.

Assignments number 1 and 3 have not been ruled out. For assignment #1, 1_{11}-2_{12} μ_a type at 5845.8 MHz and the 1_{01}-2_{02} μ_a type at 6113.8 MHz are the only predicted lines that have been searched for. They were not found. However, no μ_a type transitions have been found bringing up the possibility that only μ_b type and μ_c type transitions occur, because there is no component of μ along the a inertial axis. The next step would be to search for predicted transitions of the stronger dipole, μ_b. For assignment #3 none of the predicted transitions have been searched for. Therefore, the

next step would be to search for μ_b transitions, 1_{01}-1_{10} at 6473.2, 2_{02}-2_{11} at 6759.4, and 3_{03}-3_{12} at 7205.5 MHz.

The Ar (H_2O-HCN) system was studied with some success, however the study is not yet complete. Eleven μ_b type transitions and two μ_a type transitions were found. The lines searched for up to J=4 are summarized in Fig.1. The first line of unknown cause, was found at 4754.5 MHz and eventually it was noticed that its intensity increased with the addition of H_2O vapor to the gas pulse. Further checks showed it also needs Ar and HCN. Some potential energy calculations were made for an Ar-(H_2O-HCN) trimer, giving estimates of the three rotational constants. The 4754.5 line was assigned as a μ_b type transition, 0_{00}-1_{11}. For an asymmetric rotor the 0_{00}-1_{11} transition is at the frequency A+C. More transitions that are linearly dependent on A and C were searched for and found, giving more accurate values of A and C. The value of B was then reestimated using the original inertial defect (Δ) calculation and the values of A and C.

$$(f/A) + (f/B) - (f/C) = \Delta \qquad (4)$$

Where f is a constant=505379.07.

The 1_{11}-2_{12} transition frequency for an asymmetric rotor is B+3C. This line was searched for and found, in order to pin down a more accurate value for B. With now fairly accurate values for all three asymmetric top rotational constants the spectrum was recalculated.

Both μ_a and μ_b type transitions were found and the approximate line centers were fitted to the rotational constants. The resulting

fitted rotational constants are A=3535.7, B=1845., and C=1219.4 MHz. The calculated and observed transitions are listed in Table IV. The hfs is listed in Table V. The centrifugal distortion constants could not be fitted with sufficient accuracy. The inertial defect was recalculated to a value of 2.39.

The μ_a type transitions have larger residues than the μ_b type transitions. Also, some predicted μ_a and μ_b type transitions have been searched for without success, including the 0_{00}-1_{01}. This indicates that something in the system has not been accounted for. It could be internal rotation of the H_2O-HCN dimer coupling with the molecular rotation with the major component of the coupling along the a- inertial axis. This would lead to deviations in the predicted spectrum for both μ_b and μ_a type transitions, however, with a larger deviation in the μ_a type transitions.

The hfs could not be fitted well for most transitions. The value of the quadrupole interaction term is dependent upon the rotational level and therefore must be calculated independently for each rotational transition. The 0_{00}-1_{11} hfs has been fitted accurately. It depends only on the projection of the HCN quadrupole interaction onto the b-axis, giving a projection of 30.5°. By using the value of quadrupole interaction for free HCN and the angle between the HCN axis and the b inertial axis, $\emptyset_{zb}$, the projections onto all three inertial axis can be calculated.

$$Q_{bb}=(1/2)Q_0\langle 3\cos^2\emptyset_{zb}-1\rangle \qquad \emptyset_{zb}=30.5^\circ \qquad (5)$$

$$Q_{cc}=(1/2)Q_0\langle 3\cos^2\emptyset_{zc}-1\rangle \qquad \emptyset_{zc}=120.5^\circ \qquad (6)$$

$$Q_{aa}=(1/2)Q_0\langle 3\cos^2\emptyset_{za}-1\rangle \qquad \emptyset_{za}=90^\circ \qquad (7)$$

However, using these values in the ICI fitting program resulted in an unsuccessful fit of the hfs of other transitions.

Due to the number of predicted transitions found and their approximate fit, it is apparent that the Ar(H_2O-HCN) trimer transitions are being observed. However, inconsistencies in the fit of the line centers and hfs indicate that the structure and/ or the dynamics of the system are more than a simple, semi-rigid asymmetric trimer. No pattern has been noticed for the transitions that have not been found. More transitions need to be found in order to determine the structure adequately.

DISCUSSION

A discussion of the subunits of the $Ar(H(D)F)_2$ trimer will be included here, to lead to a discussion of possible perturbations with the addition of Ar to the H(D)F dimer.

The DF dimer exists in a nonlinear equilibrium geometry. The end DF is bent 63° ($Ø_1$) from the F-F axis. The internal DF is bent 10° ($Ø_2$) in the opposite direction. The a inertial axis is inclined to the F-F axis, making the dipole moment, μ, along the a axis. The DF dimer exhibits tunneling motion which splits the rotational levels into symmetric and antisymmetric tunneling states.

The three $Ar(DF)_2$ transitions observed exhibit tunneling. This indicates that the addition of Ar does not prevent the tunneling inversion. It is difficult to determine whether the Ar adds in the plane or out of the plane of the dimer, and how this addition perturbs the geometry of the dimer. A definite assignment and more transitions are needed to determine the structure.

The $Ar(H_2O\text{-}HCN)$ trimer can also be discussed in terms of its substituents. The H_2O-HCN dimer has an effectively planar structure, with the O and the H forming a H-bond. One water H is located above the plane while the other is located below the plane. The structural parameters are R(O-C) and Ø (the angle between the C_2 axis of the water molecule and the a axis) and O (the angle between the HCN axis and the a axis). The values are 3.157 Å, 51°, and 10° respectively. The R(O-C) is located along the b inertial axis, making the cluster dipole's major component along the b axis.

In the trimer both μ_a and μ_b type transitions have been observed, with the μ_b considerably larger. The selection rules for these dipole tranwsitions are ee-eo and oe-oo for μ_a type transitions and oo-ee and oe-oo for μ_b type transitions. More transitions of both types are needed for a structural determination.

ACKNOWLEDGEMENTS

I would like to thank Tim Germann, Tryggvi Emilsson, and Carl Chuang I would especially like to thank Dr. Gutowsky for all his help and patience.

REFERENCES

1. T.A. Dixon, C.H. Joyner, F.A. Baiocchi, and W. Klemperer, J. Chem. Phys. 74, 6539 (1981).

2. M.R. Keenan, L.W. Buxton, E.J. Campbell, A.C. Legon, and W.H. Flygare, J. Chem. Phys. 74, 2133 (1981).

3. H.S. Gutowsky, T.D. Klots, C. Chuang, C.A. Schmuttenmaer, and T. Emilsson, J. Chem. Phys. 86, 569 (1987).

4. H.S. Gutowsky, T.D. Klots, C. Chuang, J.D. Keen, C.A. Schmuttenmaer, and T. Emilsson, J. Am. Chem. Soc. 109, 5633 (1987).

5. H.S. Gutowsky, C. Chuang, T.D. Klots, T. Emilsson, R.S. Ruoff, and K.R. Krause, J. Chem. Phys. 88, 2919 (1988).

6. H.S. Gutowsky, C. Chuang, J.D. Keen, T.D. Klots, and T. Emilsson, J. Chem. Phys. 83, 2070 (1985).

7. B.J. Howard, T.R. Dyke, and W. Klemperer, J. Chem. Phys. 81, 5417 (1984).

8. A. J. Fillery-Travis, A.C. Legon, and L.C. Willoughly, Proc Roy. Soc. (London) A, 396, 405 (1984).

9. E.J. Campbell, W.G. Read, J.A. Shea, Chem. Phys. Lett. 94, 69 (1983).

Table I

Transition (MHz)	Components
3807	Ar/HF
5906.00	Ar/DF
5923.90	Ar/HF
6032.40	Ar/DF
6058.90	?
6069.47	Ar/HF
6089.32	Ar/HF
6116.57	Ar/HF
6124.87	Ar/HF
6212.30	?
6222.43	Ar/HF
6692.75	Ar/DF
9506.9	Ar/DF

Table II

Transition (MHz)	Splitting (MHz)
6010.7	1.22
6278.7	0.81
9340.0	1.22

Table III

Assignment			Rotational Constant (MHz)		
6010.7	6278.7	9340.0	A	B	C
2_{02}-$2_{12}\mu_c$	1_{01}-$1_{11}\mu_c$	0_{00}-$1_{11}\mu_b$	7974.8	1669.2	1392.2
1_{01}-$2_{02}\mu_a$	1_{10}-$2_{11}\mu_a$	0_{00}-$1_{11}\mu_b$	7965.5	1634.7	1374.6
1_{11}-$2_{12}\mu_a$	1_{01}-$2_{02}\mu_a$	0_{00}-$1_{11}\mu_b$	7906.6	1710.5	1433.4
1_{01}-$2_{02}\mu_a$	1_{10}-$2_{11}\mu_a$	0_{00}-$1_{10}\mu_c$	7705.4	1634.6	1374.8
1_{11}-$2_{12}\mu_a$	1_{01}-$2_{02}\mu_a$	0_{00}-$1_{10}\mu_c$	7629.2	1710.8	1433.3
2_{02}-$2_{11}\mu_b$	3_{03}-$3_{12}\mu_b$	0_{00}-$1_{10}\mu_c$	7503.3	1836.8	1666.6
1_{01}-$1_{10}\mu_b$	2_{02}-$2_{11}\mu_b$	0_{00}-$1_{10}\mu_c$	7545.7	1794.4	1535.0
2_{02}-$2_{12}\mu_c$	1_{01}-$1_{11}\mu_c$	2_{21}-$3_{22}\mu_c$	7973.8	1695.1	1418.2
2_{02}-$2_{11}\mu_b$	3_{03}-$3_{12}\mu_b$	2_{12}-$3_{22}\mu_a$	7308.3	1641.8	1471.6
2_{02}-$2_{11}\mu_b$	3_{03}-$3_{12}\mu_b$	3_{21}-$3_{22}\mu_a$	7437.7	1686.4	1427.0

Table IV

J_{k-k}	Observed	Calculated	Residue
1_{11}-0_{00}	4754.539	4754.911	-0.372
1_{01}-2_{12}	7191.6	7191.405	0.195
2_{21}-2_{12}	6954.6	6954.627	-0.027
3_{12}-3_{03}	4456.4	4456.347	0.053
3_{21}-3_{12}	4911.9	4912.065	-0.165
3_{03}-2_{12}	7449.3	7449.542	-0.242
3_{22}-3_{13}	7973.4	7973.388	-0.002
3_{22}-2_{11}	14262.271	14262.105	0.166
4_{13}-4_{04}	6491.5	6491.579	-0.079
5_{23}-5_{14}	5802.6	5802.558	0.042
6_{24}-6_{15}	7348.4	7349.183	-0.783*
2_{02}-1_{01}	5984.6	5983.680	0.920
2_{12}-1_{11}	5498.0	5500.553	-1.500*

* Not Included in the fit.

TABLE V

$J_{k\text{-}k}$	hfs
1_{11}-0_{00}	4753.8160
	4754.6840
	4755.9833
1_{01}-2_{12}	7190.64
	7190.85
	7191.56
	7191.77
	7192.65
2_{21}-2_{12}	6954.29
	6954.55
	6954.78
	6955.22
3_{12}-3_{03}	4455.73
	4456.53
	4456.64
	4456.77
3_{21}-3_{12}	4911.67
	4911.80
	4912.11
3_{03}-2_{12}	7449.28
	7449.40
3_{22}-3_{13}	7976.57
	7976.60

Table V (contd.)

	7976.85
	7977.05
3_{22}-2_{11}	14261.549
	14262.476
	(14262.655)
4_{13}-4_{04}	6491.10
	6491.50
	6491.53
	6493.11
5_{23}-5_{14}	5802.54
	5802.61
	5802.81
6_{24}-6_{15}	7348.40
	7348.46
2_{02}-1_{01}	5984.43
	5984.46
	5984.60
	5985.30
2_{12}-1_{11}	5498.30
	5498.72
	5499.84

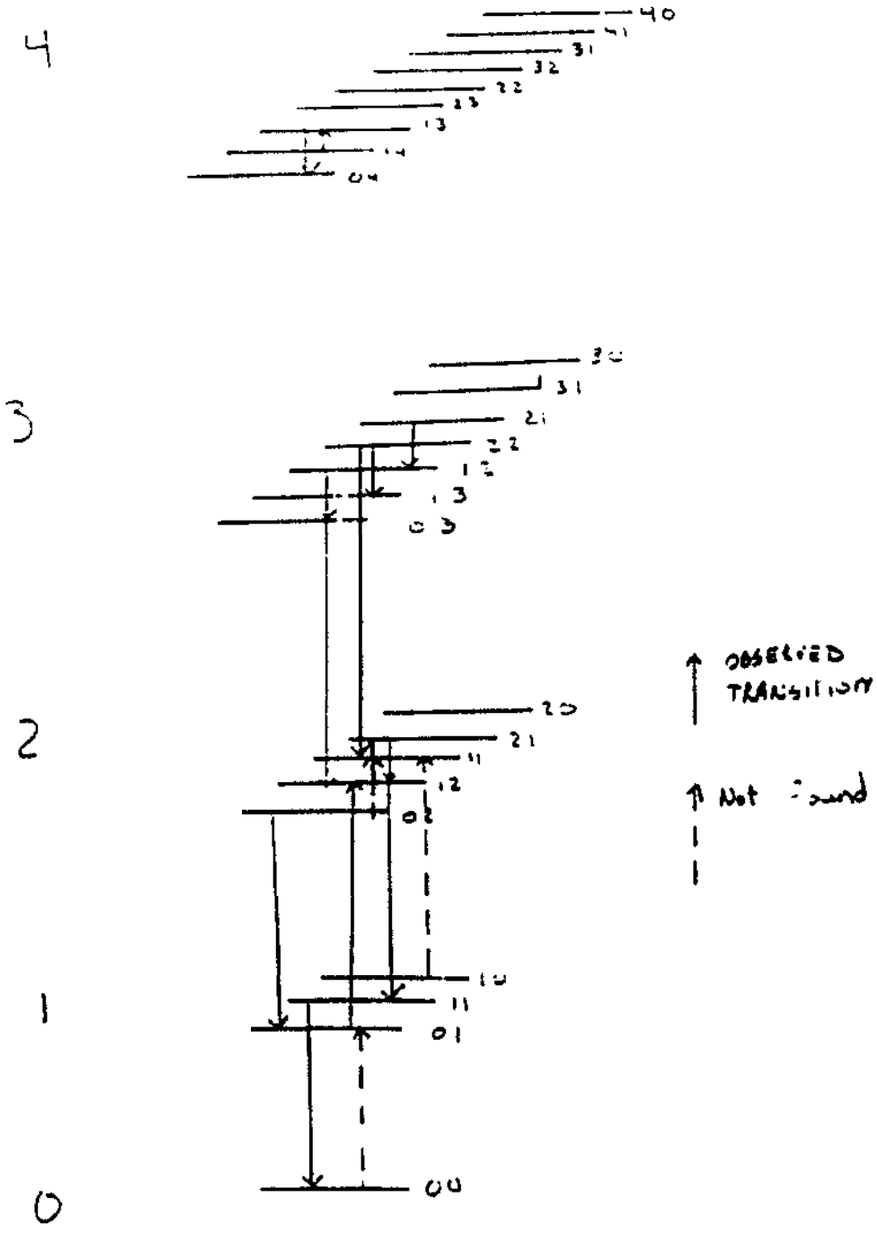
J
4
3
2
1
0
40
41
31
32
22
23
13
14
04
30
31
21
22
12
13
03
20
21
11
12
02
10
11
01
00
OBSERVED TRANSITION
Not Found

Fig 1